Published in final edited form as:
Biol Cybern. 2002 July ; 87(1): 40–49. doi:10.1007/s00422-002-0320-7.

Force and torque production in static multifinger prehension: biomechanics and control. II. Control

Vladimir M. Zatsiorsky, **Robert W. Gregory**, and **Mark L. Latash**
Department of Kinesiology, The Pennsylvania State University, University Park PA 16802, USA

Abstract

The coordination of digits during combined force/torque production tasks was further studied using the data presented in the companion paper [Zatsiorsky et al. Biol Cybern this issue, Part I]. *Optimization* was performed using as criteria the cubic norms of (a) finger forces, (b) finger forces normalized with respect to the maximal forces measured in single-finger tasks, (c) finger forces normalized with respect to the maximal forces measured in a four-finger task, and (d) finger forces normalized with respect to the maximal moments that can be generated by the fingers. All four criteria failed to predict antagonist finger moments when these moments were not imposed by the task mechanics. *Reconstruction of neural commands*: The vector of neural commands **c** was reconstructed from the equation $\mathbf{c} = \mathbf{W}^{-1}\mathbf{F}$, where **W** is the finger interconnection weight matrix and **F** is the vector of finger forces. The neural commands ranged from zero (no voluntary force production) to one (maximal voluntary contraction). For fingers producing moments counteracting the external torque ('agonist' fingers), the intensity of the neural commands was well correlated with the relative finger forces normalized to the maximal forces in a four-finger task. When fingers produced moments in the direction of the external torque ('antagonist' fingers), the relative finger forces were always larger than those expected from the intensity of the corresponding neural commands. The individual finger forces were decomposed into forces due to 'direct' commands and forces induced by enslaving effects. Optimization of the neural commands resulted in the best correspondence between actual and predicted finger forces. The antagonist moments are, at least in part, due to enslaving effects: strong commands to agonist fingers also activated antagonist fingers.

1 Introduction

This paper is a sequel to Zatsiorsky et al. (2002); it is based on the data reported in that paper and consists of three main sections: (i) optimization of finger forces, (ii) reconstruction of neural commands, and (iii) optimization of neural commands. Sections 3 and 4 are based on expanding a neural network approach previously developed for studying pressing and gripping tasks (Zatsiorsky et al. 1998) to precision grip tasks involving torque production.

Pressing and gripping tasks with several fingers have been studied to a much larger extent than torque-production tasks. In these tasks, however, the fingers act as agonists; i.e., the mechanical effects of their actions are simply summed up. The following three main phenomena have been observed: (i) *force sharing* – the total force is shared among the fingers in a specific manner (Amis 1987; Radwin et al. 1992; Li et al. 1998); (ii) *force deficit* – the maximal force produced by a given finger in a multifinger task is smaller than the force generated by this finger in a single-finger task (Ohtsuki 1981; Li et al. 1998a, b, 2000; Danion et al. 1999, 2000; Li et al. 2000); and (iii) *enslaving* – fingers that are not required to produce any force by instruction

Correspondence to: V.M. Zatsiorsky (vxzl@psu.edu, Tel.: +1-814-8653445, Fax: +1-814-8652440).

are involuntarily activated (Li et al. 1998a; Latash et al. 1998; Zatsiorsky et al. 1998, 2000). Enslaving effects reveal the existing biomechanical and neurophysiological interconnections among the fingers: a neural command to one finger induces activation of other fingers (cf. Schieber 1991, 1996; Hager-Ross and Schieber 2000).

The interdependence among fingers during force production has been addressed in our previous research (Zatsiorsky et al. 1998; Li et al. 2002). Subjects were instructed to press as hard as possible on force sensors with either one, two, three, or four fingers acting in parallel, using all possible combinations. A neural network model simulating the muscular apparatus of the hand was developed. During modeling, the input values (*neural commands*) were set either at 1 if the finger was intended to produce force or 0 if the finger was not intended to produce force. The neural network yielded a relation between the neural commands and the individual finger forces (see the Appendix). The relation between the commands and the finger forces was expressed as a matrix equation:

$$\mathbf{F}=\mathbf{w}\boldsymbol{c}/n+\mathbf{v}\boldsymbol{c} \tag{1}$$

where **F** is the (4 × 1) vector of the finger forces, **w** is the (4 × 4) matrix of weight coefficients (the matrix models interconnections among the fingers, both peripheral connections – at the muscle-tendon level – and central), ***c*** is the (4 × 1) vector of the dimensionless neural commands (a single element of the vector represents the intensity of the command sent to a given finger), **v** is the (4 × 4) diagonal matrix with gain coefficients that model the input–output relations for single-digit muscles, and *n* is the number of fingers that are intended to produce force. For a given *n*, (1) can be reduced to

$$\mathbf{F}=\mathbf{W}\mathbf{c} \tag{2}$$

From (2) it follows that a command $\mathbf{c}_i$ sent to a finger *i* (*i* = 1, 2, 3, 4) activates all other fingers to a certain extent (*enslaving effects*). A force exerted by finger *i* arises from a summation of the command sent to this finger and commands sent to other fingers. It is not clear whether these enslaving effects play a role in torque-production tasks.

The goal of the present study was to explore prehension tasks requiring simultaneous exertion of force and torque on a handheld object.

2 Optimization of finger forces

To test whether the observed force-sharing patterns (see Zatsiorsky et al. 2002) were optimal, optimization methods have been employed. The norms of the following vectors were used as cost functions:

1. Finger forces

$$G_1=\left(\sum_{i=1}^{i=4}(F_i)^p\right)^{1/p}\rightarrow \min \tag{3}$$

2. Finger forces normalized with respect to the maximal forces measured in single-finger tasks

$$G_2=\left(\sum_{i=1}^{i=4}\left(\frac{F_i}{F_{i(\max)}}\right)^p\right)^{1/p}\rightarrow \min \tag{4}$$

3. Finger forces normalized with respect to the maximal forces measured in a four-finger (index, middle, ring, and little; IMRL) task

$$G_3=\left(\sum_{i=1}^{i=4}\left(\frac{F_i}{F_{i(\mathrm{IMRL})}}\right)^p\right)^{1/p}\rightarrow \min \tag{5}$$

4. Finger forces normalized with respect to the maximal moments that can be generated by the fingers while grasping an object with four fingers

$$G_4=\left(\sum_{i=1}^{i=4}\left(\frac{F_i}{d_iF_{i(\mathrm{IMRL})}}\right)^p\right)^{1/p}\rightarrow \min \tag{6}$$

using the following constraints:

$$F_{\mathrm{tot}}>F_{\mathrm{s1}};F_i\le F_{i\max};M_{\mathrm{tot}}=\sum F_id_i=\text{const.};d_i=\text{const.} \tag{7}$$

where F_{tot} is the total of the normal finger forces; F_{sl} is the minimal grasp force necessary to prevent an object from slipping out of the hand; F_i is the force produced by an individual finger; M_{tot} is the total moment generated by the four normal finger forces; and d_i is the finger moment arm, which is the projected distance between the centers of the finger sensor and the thumb sensor (for the 'central' fingers, d_i = 12.5 mm; for the 'peripheral' fingers, d_i = 37.5 mm). Because the shear force changes as a function of the external torque (see Fig. 2 in Zatsiorsky et al. 2002), F_{sl} is different for each load/torque combination. The slip force F_{sl} was estimated as

$$F_{\mathrm{s1}}=F_{\mathrm{shear}}/\mu \tag{8}$$

where F_{shear} is the largest shear force – either the thumb or all four fingers combined – for a given load/torque combination, and μ is the coefficient of friction. The thumb shear force was measured and the shear forces of the fingers were computed as the difference between the total weight of the apparatus (the handle/beam apparatus plus the external load) minus the thumb shear force. The optimization computations were performed in MAT-LAB (Mathworks, Natick, Mass) using the 'fmincon' function, which accomplishes multidimensional constrained nonlinear optimization. The power value of the cost functions was selected to be p = 3 (values of p ranging from 1 to 15 have also been employed, but the results will not be presented here). When p = 3 criteria G_2, and G_3 are analogous to the minimum fatigue criterion

$$G_{\mathrm{fatigue}}=\sum_{i=1}^{9}(F_i/\mathrm{PCSA}_i)^p\rightarrow \min,\quad p=2,3,4 \tag{9}$$

suggested by Crowninshield and Brand (1981) for the muscle-sharing problem, which is the problem of distributing activity among synergistic muscles contributing to a joint moment. In

(9), G_{fatigue} is the so-called muscle fatigue function, where PCSA_i is the physiological cross-sectional area of the *i*th muscle, and the constant *p* was derived from the experimentally obtained relationship between muscle stress (*F*/PCSA) and endurance time of human muscles ($p = 3$ on average). Criterion G_{fatigue} is broadly used for studying the muscle-sharing problem (for recent reviews see Tsirakos et al. 1997; Prilutsky 2000; Prilutsky and Zatsiorsky 2002).

The optimization results were similar, with some small differences, for all four cost functions. For zero torque conditions, all four criteria predicted equal involvement of the finger pairs that produce pronation and supination moments, as should be expected (Fig. 1).

For nonzero torque conditions, none of the cost functions predicted antagonist moments of force, with the exception of the 2.0 kg/0.375 Nm load/torque combination (Fig. 2). This 'large load/small torque' combination evidently corresponds to zone A of the three-zone model that was introduced in Zatsiorsky et al. (2002), a zone where antagonist moments are a mechanical necessity. Hence, criteria based on minimization of finger forces fail to predict the existing antagonist moments observed in zones B and C, where they are not mechanically necessary. According to these criteria, the force distribution patterns employed by the subjects were not optimal.

3 Reconstruction of neural commands

Due to finger enslaving (Zatsiorsky et al. 1998,2000), a flexion command sent to a finger causes force production by other fingers. Equation (2) represents this fact.

3.1 Method of reconstruction and results

If the vector of finger forces **F** and weight matrix **W** are known, the vector of the neural commands can be determined by inverting (2):

$$\boldsymbol{c}=\mathbf{W}^{-1}\boldsymbol{F} \tag{10}$$

The vector $\boldsymbol{F}$ was measured in this study. The weight matrix **W** was taken from our previous study on neural network modeling of force production by several fingers (Zatsiorsky et al. 1998); please refer to (A3) in the Appendix.

In the study by Zatsiorsky et al. (1998), the group average of the sum of the individual maximal finger forces was 141.8 N. In the present study, the subjects were stronger on average; the sum of the individual finger forces was 178.2 N. Therefore, a correction coefficient of 178.2/141.8 =1.2566 was introduced and the weight matrix **W** was multiplied by this coefficient. The adjusted matrix ${}_{\text{a}}\mathbf{W}$ is

$${}_{\text{a}}\mathbf{W}=\mathbf{W}\times 1.2566=\begin{bmatrix} 31.509 & 2.859 & 1.194 & 1.162 \\ 4.461 & 21.802 & 4.272 & 1.100 \\ 2.827 & 6.346 & 17.467 & 2.859 \\ 2.765 & 2.388 & 5.026 & 14.451 \end{bmatrix} \tag{11}$$

The elements of the matrix are the finger forces induced by neural commands of maximal intensity (c_j 1). In particular: (i) any element on the main diagonal is equal to the force produced by finger *i* (*i* = 1, 2, 3, 4) induced by a command of unit intensity to this finger; for instance, a command to the index finger $\mathbf{c}_{\text{index}} = 1$ results in a force of 31.5 N; (ii) the rows of the matrix represent the force of a given finger induced by commands to all the fingers; for example, when commands of unit intensity are sent to all of the fingers the little finger generates a force of 2.765 + 2.388 + 14.451 = 24.63 N, of which only 14.5 N comes from the command sent to this

finger and the remaining 2.765 + 2.388 + 5.026 = 10.179 N are due enslaving; and (iii) the columns of the matrix correspond to the effect of a command $\mathbf{c}_i = 1$ on all four fingers. For instance, the second column represents the finger forces induced by a command of unit intensity sent to the middle finger. Such a command results in forces of 2.859 N, 21.802 N, 6.346 N and 2.388 N being produced by the index, middle, ring, and little fingers, respectively. Any element *ij* of the matrix is equal to the force of finger *i* in response to a maximal command sent to finger *j* ($\mathbf{c}_j = 1$).

The inverse of the weight matrix is

$$ {}_{a}\mathbf{W}^{-1} = \begin{bmatrix} 0.0325 & -0.0038 & -0.0007 & -0.0022 \\ -0.0060 & 0.0501 & -0.0116 & -0.0010 \\ -0.0024 & -0.0173 & 0.0649 & -0.0113 \\ -0.0044 & -0.0015 & -0.0205 & 0.0737 \end{bmatrix} \quad (12) $$

The neural commands computed from (10) are presented in Table 1.

The obtained commands, as was expected, generally ranged from 0 to 1. In one case, a command to the little finger during a supination effort somewhat exceeded one (1.037). For the large supination moments, the commands to the index finger were slightly below zero, which may represent a small extension command, or simply be a result of inaccuracies in the modeling. Taking into account that the neural command intensities were computed by combining the results of three experiments: (i) the study of Zatsiorsky et al. (1998), (ii) force measurements during torque production tasks, and (iii) maximal force measurements (Zatsiorsky et al. 2002), the accuracy of the reconstruction can be considered to be reasonable. Commands to individual fingers changed systematically with the magnitude and direction of the external torques. During the largest pronation efforts (counterbalancing an external clockwise torque of −1.5 Nm), the commands to the index finger varied from 0.658 to 0.694, i.e. the index finger was never maximally activated. However, during the largest supination efforts (counterbalancing an external counterclockwise torque of 1.5 Nm) the little finger was activated close to maximum, $c_i = 0.948–1.037$.

3.2 Neural commands and finger forces

The relationship between neural command intensities and finger forces (expressed as a percentage of the maximal force in a single-finger task) are presented in Fig. 3. When fingers produced agonist moments, the intensity of the commands was larger than the relative force while the opposite was true for the production of antagonist moments. The point at which the curves intersected was close to, but not exactly at, zero torque.

When finger forces were expressed as a percentage of the maximal forces measured in a four-finger task, the correspondence between the command intensity and the relative finger forces improved (Fig. 4).

The obtained improvement is evidently due to enslaving effects that are neglected in criteria G_1, G_2, G_3, and G_4 but are accounted for in the neural command approach. The relative contribution of the enslaving effects into the finger forces is relatively larger when a finger serves as a torque antagonist and produces a smaller force.

3.3 Decomposition of finger forces: exploration of enslaving effects

The force generated by a finger arises from the command sent to this finger (‘direct’ finger force) as well as from the commands sent to other fingers (enslaved force). The direct finger

forces can be computed as the product $w_{ii}\mathbf{c}_i$ (i = 1, 2, 3, 4), where w_{ii} is a diagonal element of the weight matrix (Fig. 5).

The difference between the actual and 'direct' forces represents enslaving effects; i.e., the force generated by a finger due to the commands sent to other fingers. The enslaved forces are presented in Fig. 6.

For the middle, ring, and little fingers, the minimum enslaved force occurs at zero torque or close to it. It is interesting to note that a rather irregular behavior of the middle finger forces (Fig. 5) is associated with a smooth, regular dependence of the enslaved forces resulting from the external torque (Fig. 6). The method allows for partitioning the effects on individual fingers due to the commands sent to each of the fingers. An example of such a decomposition for the middle finger forces is presented in Fig. 7. The summed effects from the index, ring, and little fingers are equal to the enslaved force (r = 998).

4 Optimization of central commands

The following objective function was optimized:

$$G_5=\left(\sum_{i=1}^{i=4}(\mathbf{c}_i)^p\right)^{1/p}\rightarrow \min \quad (p=1,2,\ldots,15) \tag{13}$$

where the constraint $\mathbf{c} = {}_{a}\mathbf{W}^{-1}\boldsymbol{F}$ was used in addition to the previously mentioned constraints (7). Root-meansquare (RMS) error was used as a measure of performance of this and other criteria. Overall, the G_5 criterion worked much better than the four criteria based on minimization of finger forces; in all 32 load/torque combinations with nonzero external torques, the RMS values were smaller for the neural command optimization (Table 2). On average, the RMS values for the cost function based on the neural commands equaled only 34–57% of the RMS for the other four criteria. In addition, criterion G_5 always predicted antagonist moments while the other criteria, with a few exceptions, failed to predict them (see Fig. 2). An evident reason for the better performance of the criterion based on neural commands is that the G_5 criterion accounts for enslaving effects while the other criteria do not.

5 Discussion

This study has demonstrated that phenomena such as force deficit and enslaving originally discovered in maximal pressing tasks also exist in submaximal precision grip tasks involving torque production. In this context, we imply during force deficit the necessity to use a larger command to a digit in order to produce a fixed level of force when another digit is recruited, as compared to force production by the first digit alone. The interfinger weight matrices serve as quantitative estimates of the force deficit and enslaving. The force deficit is accounted for by a coefficient 1/n, where n is the number of fingers involved in the task (see Eqs. 1 and 2) and enslaving is represented by the elements of the matrix. The inter-connection matrices relate neural commands with finger forces and allow for reconstruction of the neural commands from known values of the finger forces.

5.1 The reasons behind antagonists moments

Zatsiorsky et al. (2002) introduced a three-zone model for prehension. Antagonist moments in zone A are mechanically necessary; the reasons for their existence in zones B and C are less evident. One of the possible mechanisms causing antagonist moments in zones B and C is enslaving; antagonist fingers are activated because strong commands are sent to agonist fingers

and antagonist fingers are enslaved by these commands. The computation of the neural commands and their effects (Figs. 4–7) supports this hypothesis. The neural commands to antagonist fingers produced in response to large external torques are close to zero or even negative; for example, the neural commands to the index finger are negative in the 1.125 Nm and 1.5 Nm conditions. Nevertheless, the antagonist fingers are active and generate force due to enslaving.

A second mechanism – purely hypothetical at this point – may also contribute to the generation of antagonist moments. The experimental tasks used in this study required a high degree of accuracy; subjects were asked to maintain the vertical orientation of the handle. Antagonist muscles are usually active during static precision tasks (Flanders and Soechting 1990; Buchanan and Lloyd 1995). The coactivation of the muscles that serve the opposite movements at a joint (e.g., flexion–extension) increases the apparent joint stiffness, i.e., the resistance of the joint to the perturbation (however, see Burnett et al. 2000). It seems reasonable to assume that antagonist moments are generated because of similar reasons, namely to improve the accuracy of the system and increase its resistance to perturbations. This hypothesis can be tested by changing the accuracy requirements of the task, e.g., allow deviation of the handle up to 10° from vertical and/or by changing the moment of inertia of the apparatus.

5.2 What are neural commands?

In Zatsiorsky et al. (1998), as well as in this study, neural commands were introduced in a purely operational way, by describing the techniques employed for computing the commands. The commands are sets of neural parameters (something that we do not know) that assume a maximal value (one) when maximal voluntary contraction is required and a minimal value (zero) when voluntary force is not exerted. Because matrix methods are used for describing the relationship between commands and forces, the relationships are also implicitly assumed to be linear. The methods used in this study do not provide a means for establishing the actual physiological mechanisms behind these abstract concepts.

Neural commands, however, may have real physiological meaning. Tax and Denier van der Gon (1991) suggest that muscle force may linearly depend on neural control signals without violating such known phenomena as the size principle (Henneman et al. 1965) and nonlinear twitch summation (Burke et al. 1976). Consider a motoneuron pool that receives input from a nerve bundle. A weighted sum of activities in a nerve bundle is

$$\mathbf{I}=\sum_i \boldsymbol{u}_i \boldsymbol{e}_i \tag{14}$$

where **I** is the control signal of the motoneuron pool, $\mathbf{e}_i$ is the firing frequency of action potentials traveling along each nerve fiber in the bundle, and $\mathbf{u}_i$ is the synaptic weight of a nerve fiber *i* projecting to a motoneuron (in the model, it is assumed that synaptic weights for all motoneurons are equal). When some commonly accepted physiological facts were incorporated into the model (i.e., different recruitment density of small and large motor units) a linear relationship between a control signal **I** and the force produced by a muscle was established. Hence, the control signal **I** is proportional to the muscle force and can be interpreted as an internal representation of muscle force. While the neurophysiological mechanisms of the neural commands analyzed in this study remain unclear, there is a certain similarity between these commands and the control signals to the motoneuron pools (14).

5.3 Interfinger weight matrices

The interfinger weight matrix **W** worked remarkably well in this study; in particular the neural commands were determined with sufficient accuracy. This performance deserves to be pointed out because, as previously mentioned, the computation of the neural commands was based on empirical data from three separate experiments performed on two groups of subjects (Zatsiorsky et al. 1998 and this study). This implies that the matrix is robust and, after a necessary adjustment for differences in the strength of the subject groups, may be used for different populations. Obviously, this claim needs to be tested experimentally. In the future, it seems reasonable to use normalized weight matrices (per 1 N of total finger force measured in single-finger tasks):

$$ {}_{\mathrm{n}}\mathbf{W}=\frac{1}{\sum F_i\,(\max)}\mathbf{W} \tag{15}$$

The interfinger weight matrix **W** introduced in (2) models enslaving effects, while (1) models both enslaving and force deficit. It seems reasonable to use for analyzing these effects the set theory (Venn diagrams). For instance, let *I* and *M* be anatomical objects affecting the magnitude of the forces produced by the index and middle fingers, respectively. The objects can be muscle bundles, individual muscles, motoneuron pools, or populations of supra-spinal neurons. The $I \cap M$ intersection represents an overlap of the anatomical objects serving two fingers, for instance the muscle bundles in the extrinsic hand muscles that serve both fingers. Then, if the intersection of the sets *I* and *M* is not empty ($I \cap M \neq 0$), the union of *I* and *M* contains a smaller number of elements than *I* and *M* combined; i.e., $Card\,(I \cup M) < [Card\,(I) + Card\,(M)]$, where *Card* is the cardinality of a set. While it seems logical to assume that the intersection $I \cap M$ specifies the amount of enslaving and the difference $[Card\,(I) + Card\,(M)] - Card(I \cup M)$ specifies the amount of deficit, the situation is more complex: no correlation between the magnitude of force enslaving and force deficit in various tasks has been observed (F. Danion, personal communication, 2001).

Recent research shows that muscle bundles as well as individual muscles are not very good candidates for explaining enslaving effects. This conclusion follows from experiments in which the site of finger force application was varied and the forces were exerted either at the distal or proximal phalanges (Li et al. 2001). When the point of force application is at the distal phalanx, the extrinsic flexor muscles are the major contributors to finger force production; however, when the force of application is at the proximal phalanx the intrinsic muscle group is the major contributor. In spite of different muscle involvement, enslaving does not depend on the site of force application and is approximately the same when the forces are exerted at the distal or proximal phalanges (Zatsiorsky et al. 2000). It seems that it is not the musculotendinous interconnections, but rather higher-order interactions that define enslaving effects.

In the human primary somatosensory cortex, cortical digit representations are arranged from the lateral inferior to the medial superior aspect in anatomical order: the thumb, index finger, middle finger, ring finger, and little finger (Baumgartner et al. 1991). However, the volumes representing individual fingers overlap extensively (Krause et al. 2001). In the primary motor cortex of monkeys, neuronal populations activated by movements of different fingers also overlap in their spatial locations (Schieber and Hibbard 1993). The control of any finger movement utilizes a distributed population of neurons and the entire neuronal population activity specifies particular finger movements (Georgopoulos et al. 1999). It appears that force deficit and enslaving have their origin at this level, rather than being completely defined by musculotendinous connections at the peripheral level. It would be interesting to trace the

relationship – if it exists – between the interfinger connection matrices and the overlapping volumes of population neurons.

5.4 Finger redundancy and muscle redundancy

There is a certain similarity between finger coordination in multifinger manipulative tasks and muscle coordination in joint moment production (Li et al. 1998a). Both fingers and muscles work in parallel (Mussa-Ivaldi 1986; Zatsiorsky 2002). In statics, parallel systems are redundant and described by underdetermined sets of equations: the number of unknowns is larger than the number of available equations. For instance, the number of muscles typically exceeds the number of degrees of freedom at a joint. In kinematics, parallel systems are overconstrained and described by overdetermined sets of equations: the number of equations exceeds the number of unknowns. For instance, if the length of one singlejoint muscle is known, the joint angle and lengths of the other muscles spanning that joint can be determined. In a similar way, for a given grasp, the same force and torque can be exerted on the object by a different combination of digit forces while the position of a digit is uniquely defined by the position of the other fingers.

The evident similarities between the two systems inspire one to question whether or not the central nervous system controls these mechanically similar systems in a similar way. Note that studying finger coordination is an advantageous method for studying the force-sharing problem; contrary to the direct measurement of muscle forces, finger forces can be measured without difficulty. In particular, the question arises whether enslaving exists at the level of muscles. In other words, can the central controller activate one muscle in isolation without activating other muscles? Note that in numerous publications on the so-called muscle-sharing problem (for reviews, see Tsirakos et al. 1997; Prilutsky 2000), possible enslaving is completely neglected when different optimization methods are used. Our results question this approach.

Acknowledgments

The authors are grateful to Drs. Boris Prilutsky and Zong-Ming Li for insightful comments on the earlier versions of the manuscript. We also thank Dr. Arkady Tempelman for useful mathematical consultations and Marina Tempelman for technical help. These experiments were partly supported by NIH grants NS-35032 and AG-18751.

Appendix: Neural network modeling of finger forces: interfinger connection matrices (from Zatsiorsky et al. 1998; Li et al. 2002)

The model (Fig. A1) consists of three layers: (i) the input layer that models a central neural drive, (ii) the hidden layer that simulates transformation of the central drive into an input signal to the muscles serving several fingers simultaneously (e.g., multidigit muscles), and (iii) the output layer representing finger force output. The output of the hidden layer is set inversely proportional to the number of fingers involved. The network also features direct connections between the input and output layers that represent signals to the hand muscles serving individual fingers (e.g., single-digit muscles). During modeling, the input values (*central commands*) were set either at 1 if the finger was intended to produce force or 0 if the finger was not intended to produce force.

The neural network yielded a relation between the central commands and the individual finger forces. The relation between the central commands and the finger forces was expressed as a matrix equation:

$$\boldsymbol{F}=\mathbf{W}\boldsymbol{c}/n+\mathbf{v}\boldsymbol{c} \tag{A1}$$

where $\boldsymbol{F}$ is a (4 × 1) vector of the finger forces, **w** is a (4 × 4) matrix of weight coefficients (the matrix models the multidigit muscles), $\boldsymbol{c}$ is a (4 × 1) vector of the dimensionless central commands, **v** is a (4 × 4) diagonal matrix with the gain coefficients that models the input–output relations for the single-digit muscles, and *n* is the number of fingers that are intended to produce force (for these fingers, central commands = 1). The values of **w** and **v** were found to be equal:

$$\mathbf{w}=\begin{bmatrix} 32.7 & 9.1 & 3.8 & 3.7 \\ 14.2 & 29.0 & 13.6 & 3.5 \\ 9.0 & 20.2 & 22.4 & 10.9 \\ 8.8 & 7.6 & 16.0 & 17.2 \end{bmatrix} \text{ and } \mathbf{v}=\begin{bmatrix} 16.9 & 0 & 0 & 0 \\ 0 & 10.1 & 0 & 0 \\ 0 & 0 & 8.3 & 0 \\ 0 & 0 & 0 & 7.2 \end{bmatrix} \quad \text{(A2)}$$

For *n* = 4, (A1) can be reduced to

$$\boldsymbol{F}=\mathbf{W}\boldsymbol{c}=\begin{bmatrix} 25.08 & 2.28 & 0.95 & 0.93 \\ 3.55 & 17.35 & 3.40 & 0.88 \\ 2.25 & 5.05 & 13.9 & 2.28 \\ 2.20 & 1.90 & 4.00 & 11.50 \end{bmatrix} \boldsymbol{c} \quad \text{(A3)}$$

where **W** is the (4 × 4) matrix of weight coefficients (*interfinger connection matrix*).

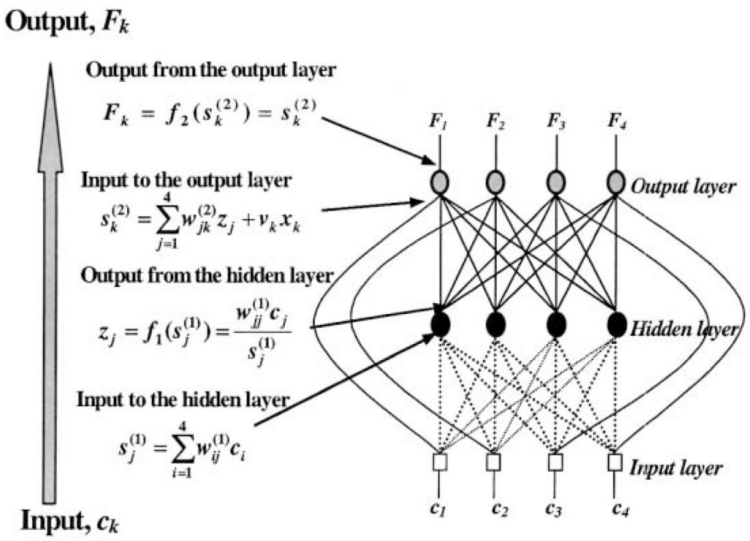

Fig. A1.

Neural network and associated mathematical formulations. The index, middle, ring, and little finger correspond to *1*, *2*, *3*, and *4*, respectively. The mathematical background of the network is explained in Zatsiorsky et al. (1998) and Li et al. (2002). The network was validated using three different training sets and worked remarkably well. In all cases, the predicted values were in the range of ± 1 SD

References

Amis AA. Variation of finger forces in maximal isometric grasp tests on a range of cylinder diameters. J Biomed Eng 1987;9:313–320. [PubMed: 3682795]

Baumgartner C, Doppelbauer A, Sutherling WW, Zeitlhofer J, Lindinger G, Lind C, Deecke L. Human somatosensory cortical finger representation as studied by combined neuromagnetic and neuroelectric measurements. Neurosci Lett 1991;134:103–108. [PubMed: 1815142]

Buchanan TS, Lloyd DG. Muscle activity is different for humans performing static tasks which require force control and position control. Neurosci Lett 1995;194:61–64. [PubMed: 7478214]

Burke RE, Rudomin P, Zajac FE. The effect of activation history on tension production by individual muscle units. Brain Res 1976;109:515–529. [PubMed: 1276932]

Burnett RA, Laidlaw DH, Enoka RM. Coactivation of the antagonist muscle does not covary with steadiness in old adults. J Appl Physiol 2000;89:61–71. [PubMed: 10904036]

Crowninshield RD, Brand RA. A physiologically based criterion of muscle force prediction in locomotion. J Biomech 1981;14:793–801. [PubMed: 7334039]

Danion, F.; Latash, M.; Zatsiorsky, V. Effects of single and multi-finger prolonged exercise on multi-finger coordination. In: Gantchev, N.; Gantchev, GN., editors. From basic motor control to functional recovery. Drinov; Sofia: 1999. p. 353-357.

Danion F, Latash ML, Li ZM, Zatsiorsky VM. The effect of fatigue on multifinger co-ordination in force production tasks in humans. J Physiol (Lond) 2000;523:523–532. [PubMed: 10699094]

Flanders M, Soechting JF. Arm muscle activation for static forces in three-dimensional space. J Neurophysiol 1990;64:1818–1837. [PubMed: 2074466]

Georgopoulos AP, Pellizzer G, Poliakov AV, Schieber MH. Neural coding of finger and wrist movements. J Comput Neurosci 1999;6:279–288. [PubMed: 10406138]

Hager-Ross C, Schieber MH. Quantifying the independence of human finger movements: comparisons of digits, hands, and movement frequencies. J Neurosci 2000;20:8542–8550. [PubMed: 11069962]

Hennemann E, Somjen G, Carpenter DO. Functional significance of cell size in spinal motoneurons. J Physiol (Lond) 1965;28:560–580.

Krause T, Kurth R, Ruben J, Schwiemann J, Villringer K, Deuchert M, Moosmann M, Brandt S, Wolf K, Curio G, Villringer A. Representational overlap of adjacent fingers in multiple areas of human primary somatosensory cortex depends on electrical stimulus intensity: an fMRI study. Brain Res 2001;899:36–46. [PubMed: 11311865]

Latash ML, Gelfand IM, Li ZM, Zatsiorsky VM. Changes in the force-sharing pattern induced by modifications of visual feedback during force production by a set of fingers. Exp Brain Res 1998;123:255–262. [PubMed: 9860263]

Li ZM, Latash ML, Zatsiorsky VM. Force sharing among fingers as a model of the redundancy problem. Exp Brain Res 1998a;119:276–286. [PubMed: 9551828]

Li ZM, Latash ML, Newell KM, Zatsiorsky VM. Motor redundancy during maximal voluntary contraction in four-finger tasks. Exp Brain Res 1998b;122:71–77. [PubMed: 9772113]

Li S, Danion F, Latash ML, Li ZM, Zatsiorsky VM. Finger coordination and bilateral deficit during two-hand force production tasks performed by right-handed subjects. J Appl Biomech 2000;16:379–391.

Li ZM, Zatsiorsky VM, Latash ML. The effect of finger extensor mechanism on the flexor force during isometric tasks. J Biomech 2001;34:1097–1102. [PubMed: 11448702]

Li ZM, Zatsiorsky VM, Latash ML, Bose NK. Anatomically and experimentally based neural networks modeling force coordination in static multi-finger tasks. Neurocomputing. 2002 (in press).

Mussa-Ivaldi, FA. Compliance. In: Morasso, P.; Tagliasco, V., editors. Human movement understanding. North-Holland; Amsterdam: 1986. p. 159-212.

Ohtsuki T. Inhibition of individual fingers during grip strength exertion. Ergonomics 1981;24:21–36. [PubMed: 7227358]

Prilutsky BI. Coordination of two- and one-joint muscles: Functional consequences and implications for motor control. Mot Control 2000;4:1–44.

Prilutsky BI, Zatsiorsky VM. Interpretation of muscle coordination: insight from optimization-based models. Exerc Sports Sci Rev 2002;30:32–38.

Radwin R, Oh S, Jensen TR, Webster JG. External finger forces in submaximal five fingers static pinch prehension. Ergonomics 1992;35:275–288. [PubMed: 1572337]

Schieber MH. Individuated finger movements of rhesus monkeys: a means of quantifying the independence of the digits. J Neurophysiol 1991;65:1381–1391. [PubMed: 1875247]

Schieber, M. Individuated finger movements. Rejecting the labeled-line hypothesis. In: Wing, AM.; Haggard, P.; Flanagan, JR., editors. Hand and brain. Academic; San Diego: 1996. p. 81-98.

Schieber MH, Hibbard LS. How somatotopic is the motor cortex hand area? Science 1993;261:489–492. [PubMed: 8332915]

Tax AA, Denier van der Gon JJ. A model for neural control of gradation of muscle force. Biol Cybern 1991;65:227–234. [PubMed: 1932280]

Tsirakos D, Baltzopoulos V, Bartlett R. Inverse optimization: functional and physiological considerations related to the force-sharing problem. Crit Rev Biomed Eng 1997;25:371–407. [PubMed: 9505137]

Zatsiorsky, VM. Kinetics of human motion. Human Kinetics; Champaign, IL: 2002.

Zatsiorsky VM, Li ZM, Latash ML. Coordinated force production in multi-finger tasks: finger interaction and neural network modeling. Biol Cybern 1998;79:139–150. [PubMed: 9791934]

Zatsiorsky VM, Li ZM, Latash ML. Enslaving effects in multi-finger force production. Exp Brain Res 2000;131:187–195. [PubMed: 10766271]

Zatsiorsky VM, Gregory RW, Latash ML. Force and torque production in static multifinger prehension: biomechanics and Control. I. Biomechanics. Biol Cybern. 2002 (this issue).

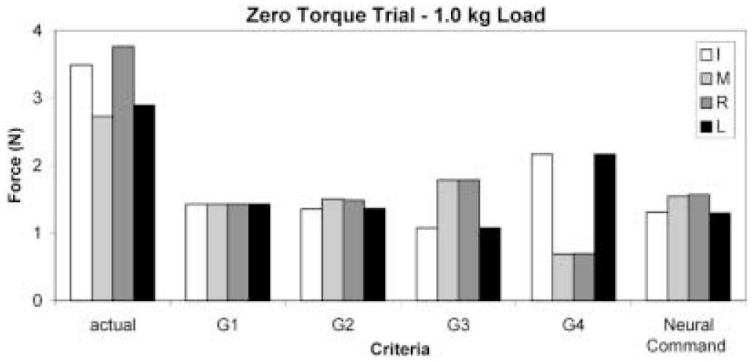

Fig. 1.

Actual and predicted (optimal) finger forces for the zero torque conditions with a 1.0 kg load. All four criteria (G_1, G_2, G_3, and G_4) predicted equal activation of the *index–middle* (*I–M*) and *ring–little* (*R–L*) pairs of fingers. Optimization of neural commands are explained and discussed in the text. Note the large difference between the actual and predicted forces; there is an unusually large *safety margin*

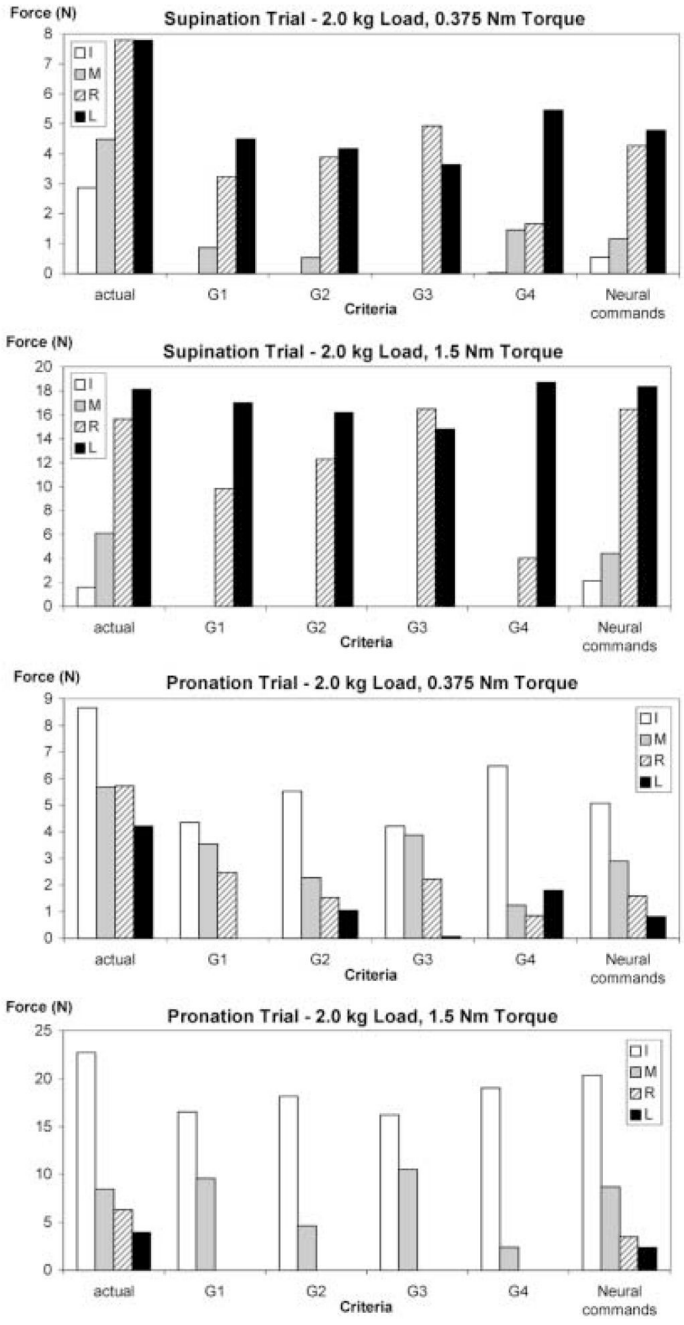

Fig. 2.

Comparison of actual force data with force patterns predicted by different optimization criteria. Criteria G_1, G_2, G_3, and G_4 predict antagonist moments only for the 2.0 kg/0.375 Nm load/torque combination

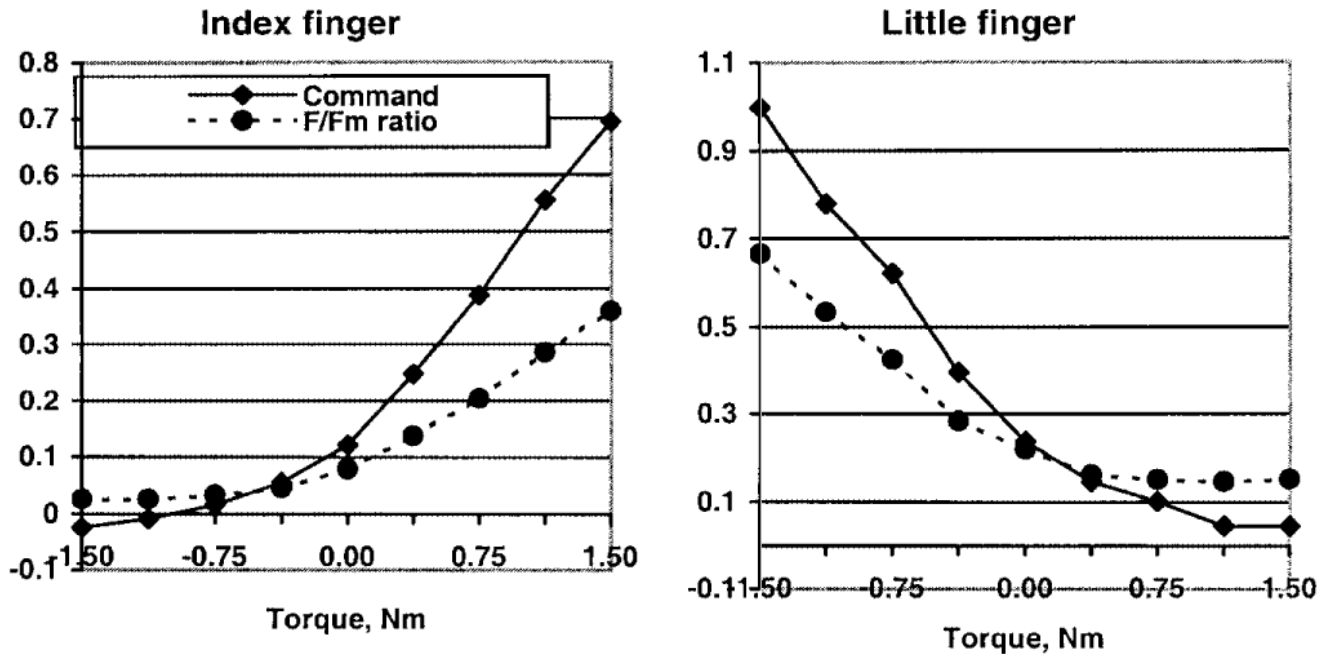

Fig. 3.

Command intensity and relative finger forces ($F_i/F_{i\max}$ ratio: finger force/maximal force in a single-finger task) for the 2.0 kg load conditions. Representative examples

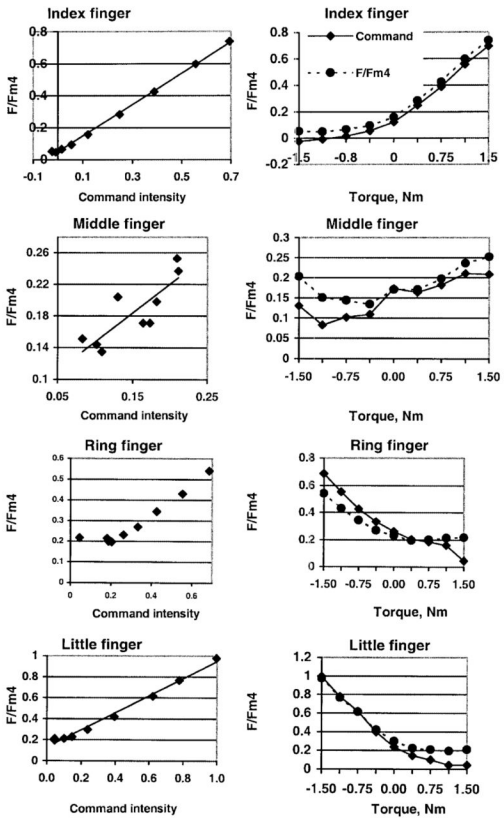

Fig. 4.

Central commands and relative finger forces (expressed as a percentage of the maximal force in a four-finger grip task) for the 2.0 kg load conditions

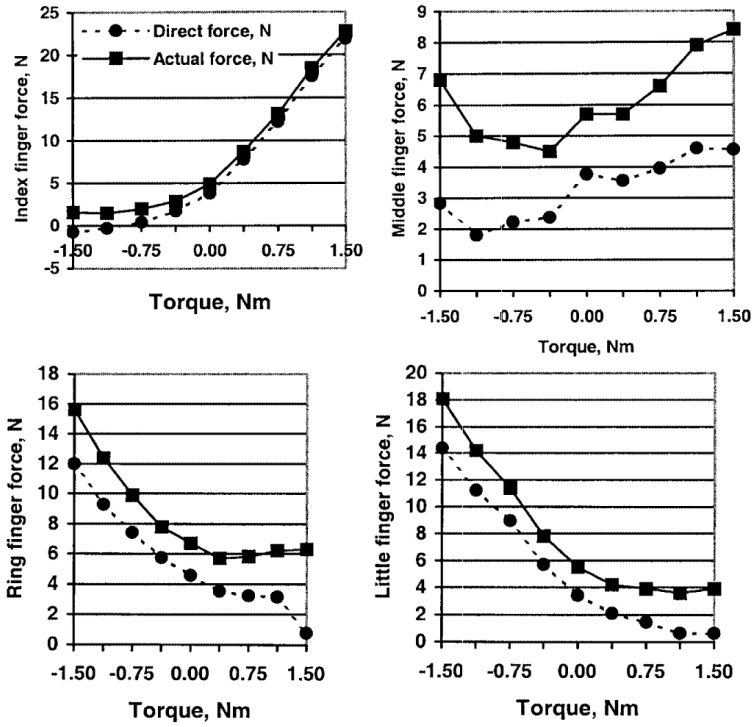

Fig. 5.

Actual and 'direct' finger forces at different external torques for a 2.0 kg load. The direct forces were computed as the products of the diagonal elements of the matrix of the connection weights w_{ii} (i = 1, 2, 3, 4) times the corresponding finger commands

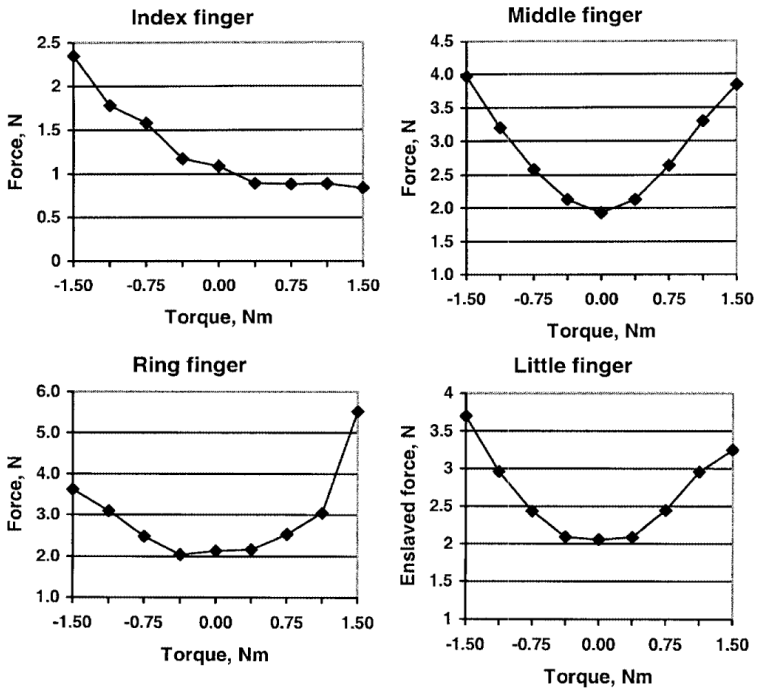

Fig. 6.
Enslaved forces (in Newtons) for a 2.0 kg load

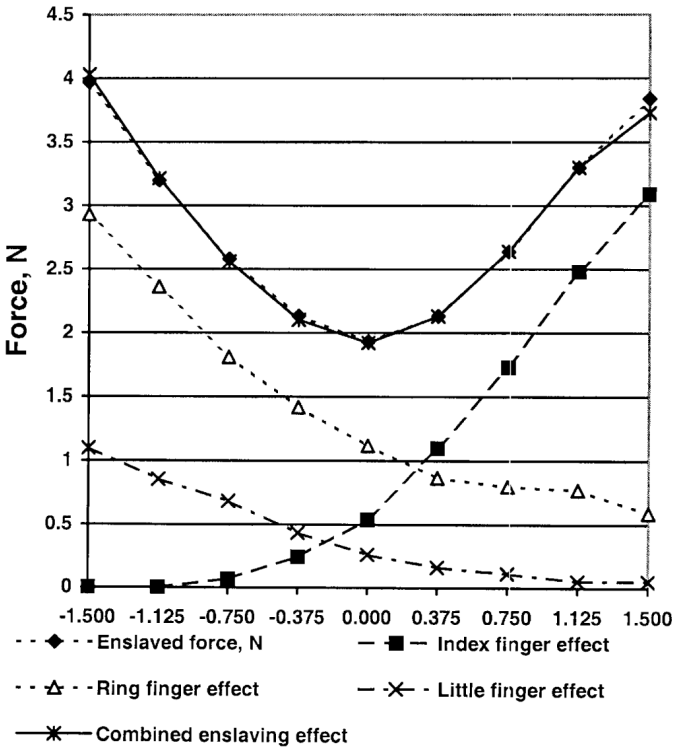

Fig. 7.
Decomposition of enslaving effects due to activation of the middle finger for a 2.0 kg load

Table 1

The neural commands to the individual fingers for the various load and torque conditions (maximal intensity = 1)

Torque, Nm	Load 0.5 kg	Load 1.0 kg	Load 1.5 kg	Load 2.0 kg
		Index finger		
−1.5	−0.035	−0.028	−0.036	−0.024
−1.125	−0.006	−0.010	−0.015	−0.009
−0.750	0.006	0.002	0.004	0.015
−0.375	0.023	0.027	0.029	0.055
0	0.074	0.094	0.117	0.121
0.375	0.215	0.21	0.231	0.248
0.750	0.375	0.378	0.385	0.388
1.125	0.490	0.531	0.516	0.556
1.5	0.689	0.661	0.658	0.694
		Middle finger		
−1.5	0.030	0.064	0.085	0.130
−1.125	0.016	0.035	0.089	0.083
−0.750	0.014	0.026	0.046	0.102
−0.375	0.023	0.043	0.074	0.109
0	0.042	0.067	0.123	0.173
0.375	0.056	0.079	0.110	0.164
0.750	0.082	0.087	0.139	0.182
1.125	0.110	0.117	0.171	0.211
1.5	0.140	0.206	0.238	0.209
		Ring finger		
−1.5	0.601	0.584	0.665	0.686
−1.125	0.415	0.449	0.470	0.553
−0.750	0.311	0.324	0.376	0.425
−0.375	0.192	0.233	0.297	0.333
0	0.105	0.158	0.201	0.262
0.375	0.077	0.110	0.155	0.203
0.750	0.067	0.127	0.131	0.187
1.125	0.055	0.082	0.142	0.161
1.5	0.044	0.093	0.129	0.045
		Little finger		
−1.5	0.948	1.037	0.959	0.997
−1.125	0.830	0.857	0.828	0.778
−0.750	0.580	0.581	0.601	0.621
−0.375	0.326	0.308	0.335	0.395
0	0.102	0.124	0.181	0.238
0.375	0.061	0.129	0.084	0.146
0.750	0.050	0.056	0.086	0.101

Torque, Nm	Load 0.5 kg	Load 1.0 kg	Load 1.5 kg	Load 2.0 kg
1.125	0.046	0.045	0.058	0.045
1.5	0.037	−0.034	0.025	0.045

Table 2

Optimization results RMS error values (*Sup*, supination; *Pro*, pronation)

Load (kg)	Torque (Nm)	G_1		G_2		G_3		G_4		G_5 neural commands	
		Sup	Pro	Sup	Pro	Sup	Pro	Sup	Pro	Sup	Pro
0.5	0.375	1.33	2.23	1.23	2.22	1.29	2.25	1.82	2.12	0.53	1.55
0.5	0.750	1.83	2.78	1.64	2.56	1.89	2.89	2.88	2.67	0.66	1.37
0.5	1.125	1.93	3.39	1.72	2.81	2.47	3.62	3.58	2.97	1.39	1.39
0.5	1.500	2.61	3.94	1.93	3.11	2.48	4.28	5.17	3.39	1.74	1.53
1.0	0.375	1.99	2.91	1.82	2.95	1.68	2.92	2.53	2.54	0.93	2.27
1.0	0.750	1.90	3.20	1.66	3.09	1.84	3.29	2.99	3.22	0.55	1.78
1.0	1.125	2.66	3.50	2.39	3.10	2.79	3.70	4.20	3.31	1.01	1.40
1.0	1.500	3.17	3.69	2.76	3.44	3.33	3.95	5.34	3.95	1.49	0.94
1.5	0.375	2.94	3.13	2.77	3.00	2.57	3.19	3.19	2.63	1.87	2.62
1.5	0.750	2.74	3.62	2.47	3.71	2.41	3.66	3.76	3.90	0.89	2.27
1.5	1.125	3.21	3.89	2.89	3.82	3.07	4.02	4.72	4.11	1.01	1.77
1.5	1.500	3.87	4.19	3.22	4.23	3.19	4.37	6.21	4.76	1.09	1.36
2.0	0.375	3.69	4.01	3.62	3.95	3.64	4.04	3.89	3.68	2.97	3.97
2.0	0.750	5.49	5.08	3.34	4.58	3.11	4.36	4.63	4.50	1.67	3.09
2.0	1.125	3.68	4.67	3.21	4.82	3.02	4.74	5.40	5.14	0.88	2.62
2.0	1.500	4.37	4.84	3.75	4.73	3.62	5.03	6.61	5.14	0.94	1.97
Average		2.96	3.69	2.53	3.50	2.65	3.77	4.18	3.63	1.22	1.99